ISSN 0020-4412, Instruments and Experimental Techniques, 2024, Vol. 67, No. 5, pp. 971–976. © Pleiades Publishing, Ltd., 2024.

GENERAL EXPERIMENTAL TECHNIQUE

Investigation of the Spectral Composition of X-Ray Radiation from Femtosecond Laser Plasma by Thermoluminescent Detectors

G. H. Salakhutdinov[a,*], K. A. Ivanov[b,c], I. G. Grigoryeva[a], V. V. Kushin[a], A. A. Rupasov[c], I. N. Tsymbalov[d], A. B. Savelyev-Trofimov[b,c], I. A. Busygina[a], and P. Yu. Naumov[a]

[a] *National Research Nuclear University MEPhI (Moscow Engineering Physics Institute), Moscow, 115409 Russia*

[b] *Moscow State University, Moscow, 119991 Russia*

[c] *Lebedev Physical Institute, Russian Academy of Sciences, Moscow, 119991 Russia*

[d] *Institute for Nuclear Research (INR), Russian Academy of Sciences, Moscow, 117312 Russia*

**e-mail: saip07@mail.ru*

Received January 10, 2024; revised January 10, 2024; accepted March 11, 2024

Abstract—A technique based on thermoluminescent LiF(Mg,Ti) lithium fluoride detectors has been developed to study the spectral composition of X-ray radiation of femtosecond laser plasma in a wide range of photon energies from 1 keV to almost 1 MeV. This technique has been experimentally tested together with matrix-type semiconductor detectors. The plasma parameters have been measured under the action of a femtosecond pulse with a peak intensity of $\sim 10^{18}$ W/cm^2 on a metal (copper) target, and good agreement is demonstrated between data from different detector types in terms of determining both the spectrum shape and the coefficient of the laser-pulse energy conversion into an X-ray flux. The temperature of hot electrons has been estimated, and its value exceeds 100 keV. The X-ray flux of copper *K*-lines, which exceeds 10^9 per shot, has been determined. The advantages and drawbacks of techniques for measuring spectra in problems of laser-plasma interaction are considered.

DOI: 10.1134/S002044122470163X

1. INTRODUCTION

The spectral composition of pulsed high-intensity X-ray radiation is studied in many fields of science and technology, including plasma physics. X-ray diagnostics of plasma objects is an important source of information about the parameters of the emitting plasma and the physical processes in it [1–5]. One of the promising types of X-ray sources with a wide spectral range is based on high-intensity laser plasma in which produced plasma is able to effectively accelerate electrons with energies from tens of keV to hundreds of MeV and generate X rays with energies above 1 MeV [1, 2]. Owing to the progress in the development of up-to-date femtosecond laser facilities capable of generating pulses with a high repetition rate and high peak power, laser-plasma X-ray sources have found application in X-ray radiography with high spatial and time resolutions, in X-ray spectroscopy and in astrophysics [1–6].

It should be noted that, along with the sources of bremsstrahlung and characteristic radiation obtained when dense (solid [7], liquid [8], structured [9, 10]) targets are exposed to laser radiation, fully optical sources also appear in which high-energy X rays are produced during betatron oscillations of electrons [11] or in the process of Compton backscattering [12].

The peculiarity of such sources consists in the ultrashort duration of an X-ray shot, which is comparable to the duration of a laser pulse (100 fs or less) [9]. Detection of X rays is difficult under such conditions since charged particles (electrons, ions) are also produced within one short pulse. Intense electromagnetic pickup is simultaneously generated, which can produce significant interference noise at the detector output.

Different types of multichannel spectrometers are used for X-ray spectrometry of laser plasma. The principle of their operation is based on the separation of X rays of different energies in space (crystal-diffraction spectrometers), on the use of various X-ray filters (gray filters, *K*-filters, Ross filters), or on the detection of single X-ray photons. A characteristic feature of most detectors is the relatively narrow range of measured energies, which results in using several measurement channels at once. Along with this, the problem of reconstructing the spectrum from the detector readings inevitably arises, which, in addition, increases the measurement error.

The purpose of this work is to measure X-ray radiation from laser plasma produced at the surface of a

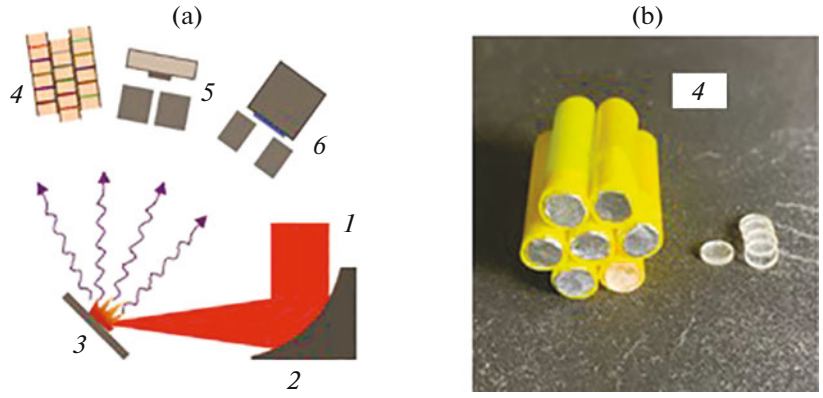

Fig. 1. (a) Schematic diagram of the experimental setup and (b) TLD array: (*1*) laser pulse, (*2*) focusing optics, (*3*) target, (*4*) TLD-based spectrometer, (*5*) MediPix detector, and (*6*) CCD array with the back illumination.

solid copper target by a femtosecond laser pulse with a peak intensity of ~10^{18} W/cm^2. A set of matrix-type semiconductor detectors was used in the measurements in the single-photon counting mode, and thermoluminescent detectors (TLDs) were used for spectrometry based on the gray filter method [13]. This has made it possible to increase the reliability of the results. X-ray spectra of femtosecond laser plasma have been obtained in the energy range $2 \le h\nu \le 800$ keV. The efficiency of energy transfer from the laser pulse to X-ray photons is evaluated. The advantages and drawbacks of the detection techniques are considered. Despite the limited energy resolution, TLDs can be used to acquire data in a certain number of laser pulses in new experiments, e.g., with petawatt-power lasers [14] or unique targets [15].

2. EXPERIMENTAL SETUP AND A MEASUREMENT TECHNIQUE

The Ti:Sa laser system of the Faculty of Physics of Moscow State University with a power of approximately 0.5 TW was used in the experiments as a source of the main laser pulse. Its characteristics were as follows: 800 nm wavelength, 10 Hz pulse repetition rate, 20 mJ maximum pulse energy at the target, and 50 fs pulse duration. The laser beam incident at the surface of the copper target at an angle of 45° to the normal was focused by an off-axis parabolic mirror ($F/D = 6$) to a spot of approximately 4 μm in diameter at half-maximum, which provided a peak intensity of 10^{18} W/cm^2. The experiments were carried out in a vacuum chamber with a residual pressure of ~10^{-2} Torr. The schematic diagram of the experimental setup is shown in Fig. 1a.

The measurement of the X-ray spectrum from the generated laser plasma was carried out by a pair of semiconductor position-sensitive detectors operating in the single-photon counting mode. This mode was attained by selecting and placing attenuation filters and collimators between the radiation source and the detector. The measurements were made in the energy range of 4–30 keV by a cooled GreatEyes 1024 1024 BI DD X-ray CCD camera with back illumination. The characteristics of the CCD camera were as follows: 40 μm thickness of the active silicon layer, 1 million pixels with a pitch of 13 μm, and ~300 eV energy resolution. A MediPix TPX2 detector with a CdTe sensor was used in the higher-energy range of 50–1000 keV. This sensor has the following characteristics: 1 mm thickness, 65000 pixels with a pitch of 55 μm, and ~10 keV energy resolution. The attenuation of the X-ray flux passing through the detector material is mainly determined by Compton scattering at X-ray energies above 100 keV. The initial plasma spectra were reconstructed using the Monte Carlo method, normalized to a single shot, and referred to a full solid angle under the assumption of an isotropic X-ray distribution in space. Figure 2 shows the spectral sensitivity curves for the semiconductor detectors in view of the used filters. Data acquisition was carried out in a series of 20000 consecutive laser shots with a pulse energy fluctuation within 20%.

In addition to the semiconductor detectors, a seven-channel small-sized noise-immune spectrometer (20 mm diameter; 20 mm length) was developed and produced based on TLDs to study the spectral composition of pulsed X-ray plasma radiation in the energy range of 2–800 keV in the integrated mode.

The operation principle of TLDs is based on the fact that charge carriers produced in them by ionizing radiation are localized in trapping centers and held in them for a long time. As a result, absorbed energy is accumulated and can be released upon additional excitation. In the case of TLDs, additional excitation is caused by heating. When an irradiated TLD sample is heated, photons are emitted (thermoluminescence) at temperatures of 240–300°C (depending on the material), and their number is proportional to the absorbed dose of ionizing radiation.

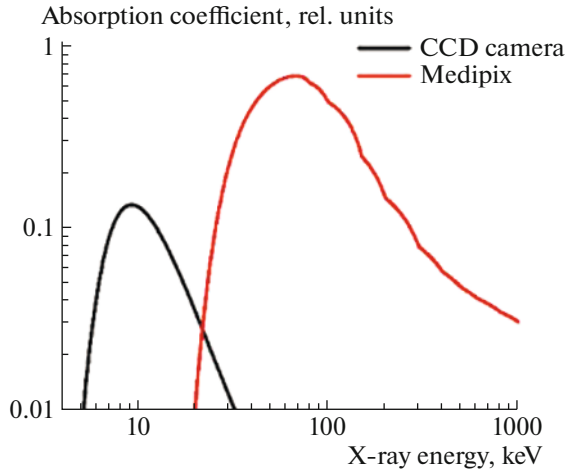

Fig. 2. Spectral sensitivity of X-ray detection for two semiconductor detectors.

A TLD is physically made in the form of a disk with a diameter of ~5 mm and a height of 0.9 mm. LiF(Mg,Ti) TLDs are immune to electromagnetic interference and UV radiation, do not have a surface dead layer, and their response is linear over a wide dynamic range of the absorbed dose (from 20 mSv to 10 Sv) [16].

The design of the developed spectrometer was the integration of seven isolated X-ray detection channels (Fig. 1b). The spectrometer channels were constructed according to the following scheme: absorption filter + detector (an array of five consecutive LiF(Mg, Ti) detectors). The arrays of LiF(Mg,Ti) detectors in a channel were fixed in place behind Al and Pb attenuation filters with different thicknesses.

The first spectrometer channel was free from an attenuation filter and was used to measure the absorbed energy J_0 from the entire X-ray spectrum of the laser plasma. Channels two to four had aluminum attenuation filters with thicknesses of 4, 32, and 60 μm, respectively. Spectrometer channels five to seven had lead attenuation filters with thicknesses of 1, 4, and 6 mm, respectively. The channels with aluminum and lead attenuation filters measured the energy of X rays emitted by the plasma and absorbed in the detectors after passing through the Al (J_{Al}) and Pb (J_{Pb}) attenuation filters, respectively. The attenuation curves shown in Figs. 3a and 3b (J_{Al}/J_0, J_{Pb}/J_0) were constructed according to the data read out of the channels with Al and Pb attenuation filters, respectively. The attenuation curve in Fig. 3c is based on the data from the lithium fluoride LiF(Mg, Ti) detectors of the first spectrometer channel.

The LiF(Mg, Ti) TLDs simultaneously acted as filters for measuring the attenuation curve in the first channel. The algorithm used to construct the attenuation curve in Fig. 3c was described in detail in [17–19]. The attenuation curve was constructed by the TLD readings in view of the TLD thickness. The first point at the attenuation curve corresponds to the total signal ΣJ_{LiF} from all TLDs with a zero absorption thickness. The second point on the attenuation curve corresponds to the total signal from all TLDs minus the signal from the first detector whose thickness is the attenuation thickness in this case. The third point on the attenuation curve corresponds to the total signal from all TLDs minus the signals of the first and second detectors, etc. The attenuation curve $J_{LiF}/\Sigma J_{LiF}$ was thereby constructed (Fig. 3c).

Absorption filters made of aluminum were used to measure the spectrum in a softer range (2–15 keV). The readings of lithium fluoride LiF(Mg,Ti) detectors of the first spectrometer channel were used to measure the spectrum in the X-ray energy range of 10–50 keV. Absorption filters made of lead were placed in the spectrometer channels to measure the hard component of X rays (30–800 keV).

The X-ray attenuation curves measured using the filter method do not directly provide the spectrum of this radiation itself. The reconstruction of X-ray spectra from the attenuation curve measured in the experiment was carried out using the effective energy

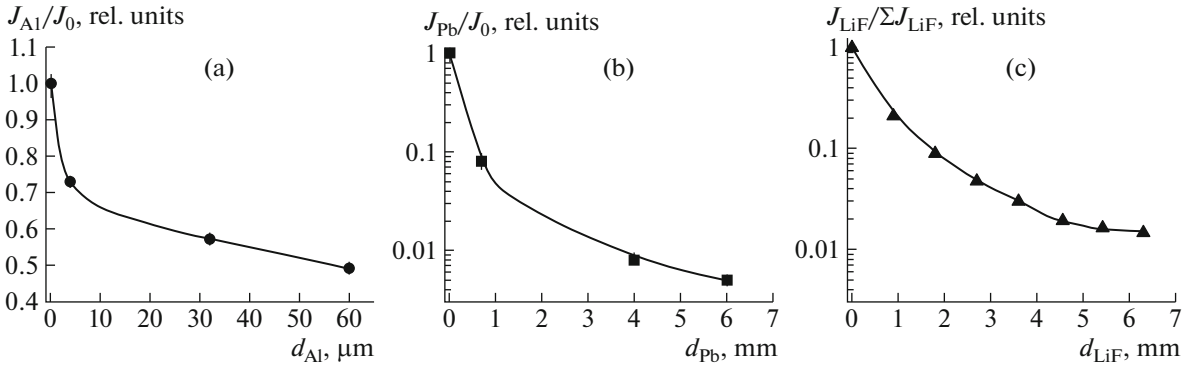

Fig. 3. Measured typical attenuation curves of filters made of (a) aluminum, (b) lead, and (c) lithium fluoride.

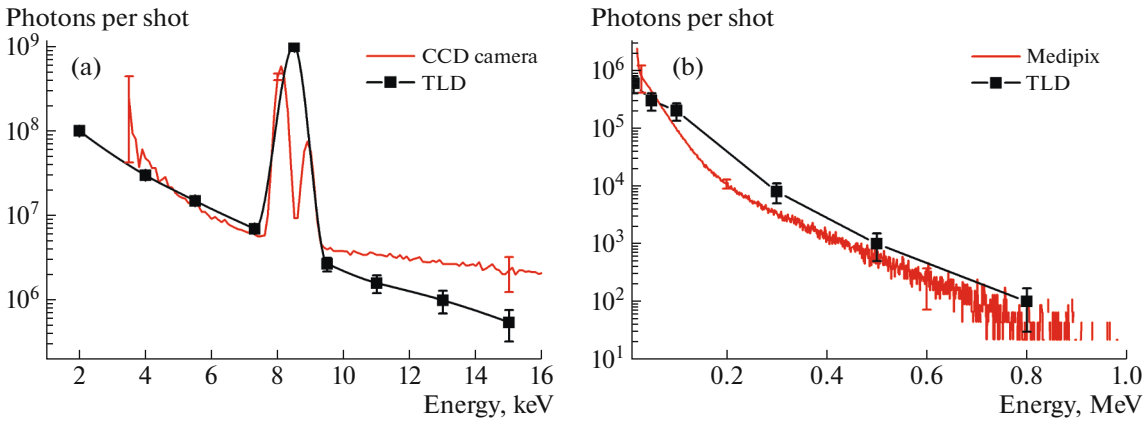

Fig. 4. Results of X-ray measurements using spectrometers based on semiconductor detectors (red curves) and LiF(Mg,Ti) detectors (black curves) in the ranges of (a) 2–15 keV and (b) 20–1000 keV.

method [16–20]. This method is based on the fact that the attenuation curve for monochromatic X rays is a linear dependence on the filter thickness, which makes it possible to determine the contribution of a certain X-ray energy to the X-ray spectrum under study.

3. RESULTS OF THE EXPERIMENT AND THEIR DISCUSSION

When a laser pulse with a peak intensity of $\sim 10^{18}$ W/cm^2 interacts with plasma of a solid target, the characteristic mechanisms of particle acceleration are collisionless: ponderomotor acceleration [21], resonant absorption, and vacuum heating [2, 22]. These mechanisms cause the appearance of a hot electron component with a quasi-temperature as high as hundreds of keV against the background of thermal electrons [1–10]. Though these fast electrons are relatively small in number [23], they are responsible not only for the emission of high-energy X rays during deceleration in the target thickness but also for the generation of characteristic radiation. Both spectral components are clearly visible in the absolute spectra measured using semiconductor detectors in different energy ranges (red curves in Fig. 4). A pair of lines corresponding to the K_α and K_β transitions of copper (8.05 and 8.9 keV, respectively) is visible in Fig. 4a. The number of X rays with an energy of 8.05 keV is as high as 5×10^9 in each laser shot, and the estimated coefficient of conversion of the pulse energy into X rays is $1.5 \pm 0.5\%$ in the range of 5–1000 keV. The temperature of the tail part of the X-ray spectrum is in good agreement with the temperature of fast electrons in the plasma, which provides a means for determining this temperature. Thus, the temperature of hot electrons T_h obtained by approximating the high-energy part of the spectrum (Fig. 4b) by a function $W(E) \sim \exp(-E/T_h)$ [24] is 115 ± 10 keV. Semiconductor detectors feature a high energy resolution (less than 500 keV for a CCD camera and approximately 10 keV for MediPix). At the same time, it is necessary that measurements be made in the mode of counting single X-ray photons using collimators and filters, which affects the data acquisition rate and the range of measured energies. The limited thickness of the sensitive layer in semiconductor detectors also determines the low detection efficiency. In the aggregate, this is reflected in the low reliability of spectrum reconstruction in the regions below 3 keV, of 10–20 keV, and over 200 keV. The spectrum envelope can nevertheless be reconstructed.

Figure 4 shows the spectra (black curves) measured by the spectrometer based on LiF(Mg, Ti) detectors, reconstructed using the effective energy method, and normalized to the full solid angle. Due to the low resolution, it is impossible to unfold the peaks of the K_α and K_β lines. Nevertheless, the spike in the readings corresponding to the characteristic X rays is reliably reconstructed. The integral X-ray flux of the K-series lines reaches 10^9, which is reasonably consistent with the data of the CCD array. According to the TLD readings, the spectrum stretches in the high-energy region to almost 800 keV, which conforms to the semiconductor detector data. The estimated temperature of hot electrons in the plasma is $\sim 100 \pm 20$ keV with a conversion coefficient of approximately 0.5% in the region of <1 MeV. The signal level is then feebly distinguishable from the noise level due to the exponential decay of the X-ray energy distribution.

An increase in the statistics would probably make it possible to detect a signal corresponding to higher-energy X rays. Nevertheless, it is important to note that the spectrum in the region below 100 keV can be measured by TLDs with high accuracy at substantially lower statistics. This is a matter of considerable interest for plasma analysis in a limited number of pulses in tasks when, e.g., unique targets (various kinds of nanostructures, foams, etc.) are used as well as when petawatt-power laser systems are used in the mode of

single pulses [25]. The lithium fluoride LiF(Mg,Ti) TLD can be placed in close proximity to the source unlike the semiconductor detectors, which makes it possible to cover a wide solid angle with a limited set of detectors and also increase the counting statistics.

Thanks to its immunity to optical radiation, the TLD has an advantage in measuring low-energy (up to 1 keV) X rays in laser-plasma experiments where the X-ray flux is codirected with optical radiation (e.g., when betatron radiation is generated). It should also be noted that TLDs are generally resistant to environmental effects and simple to use [16].

4. CONCLUSIONS

The spectral composition of the X-ray radiation of plasma produced by a femtosecond laser pulse with a peak intensity of ~10^{18} W/cm^2 at the surface of a metal target has been measured using two X-ray detection techniques. The first method consists in direct X-ray detection by matrix-type semiconductor devices in the single-photon counting mode. The second approach is based on integral measurements by LiF(Mg, Ti) TLDs using the gray filter method. After processing, the results of measurements made by both instruments have demonstrated a good agreement. The spectrum shape has been determined and the characteristic temperature of its high-energy part has been measured, which is ~100 keV. The total X-ray flux in the energy range of 2–800 keV has been established. The efficiency of converting the energy of laser radiation to X rays is ~$1.5 \pm 0.5\%$.

It has been shown that lithium fluoride LiF(Mg,Ti) TLDs are applicable to spectrometry of relativistic laser plasma and, in addition, this detection method provides reliable results. Though the energy resolution is not very high, these detectors can successfully measure the spectrum shape and estimate the temperature. The ease of use and cheapness of LiF(Mg,Ti) detectors allows the introduction of several diagnostic channels at once in the case of anisotropic X-ray distribution. It is also important to note that the immunity of LiF(Mg,Ti) detectors to optical radiation is a very important property for the detection of low-energy (up to 1 keV) X rays, for new experiments on the X-ray generation during betatron oscillations of laser-accelerated particles in a plasma channel, for diagnostics of the length of plasma channels and the peak intensity of laser radiation achieved in them by the spectra and X-ray yield, for studying the soft components in interactions of electron beams with converter targets, and in other applications.

ABBREVIATIONS AND NOTATION

TLD—thermoluminescent detector.

FUNDING

The work with thermoluminescent detectors was supported by the Priority 2030 Program of the National Research Nuclear University MEPhI. The experimental measurements of X-ray spectra and the assessment of the detector applicability to new experiments were carried out with the support of the Russian Science Foundation (project no. 22-79-10087) using equipment purchased with the support of the Science and Universities National Project of the Ministry of Education and Science of the Russian Federation.

CONFLICT OF INTEREST

The authors of this work declare that they have no conflicts of interest.

REFERENCES

1. Faure, J., Gustas, D., Guenot, D., and Bohle, F., *Plasma Phys. Control. Fus.,* 2019, vol. 61, p. 014012. https://doi.org/10.1088/1361-6587/aae047
2. Gibbon, P., *Short Pulse Laser Interactions with Matter: an Introduction,* London: Imperial College Press, 2005, p. 127.
3. Borm, B., Khaghani, D., and Neumayer, P., *Phys. Plasmas,* 2019, vol. 26, p. 023109. https://doi.org/10.1063/1.5081800
4. Barbato, F., Batani, D., Mancelli, D., Trela, J., Zeraouli, G., Boutoux, G., Neumayer, P., Atzeni, S., Schiavi, A., Volpe, L., Bagnoud, V., Brabetz, C., Zielbauer, B., Bradford, P., Woolsey, N., Borm, B., and Antonelli, L., *J. Instrum.,* 2019, vol. 14, p. C03005. https://doi.org/10.1088/1748-0221/14/03/C03005
5. Kryukov, P.G., *Usp. Fiz. Nauk,* 2015, vol. 185, no. 8, p. 817. https://doi.org/10.3367/UFNr.0185.201508b.0817
6. Ivanov, K.A., Gavrilin, M., and Volkov, R.V., *Laser Phys. Lett.,* 2021, vol. 18, p. 075401. https://doi.org/10.1088/1612-202x/ac034a
7. Huang, K., Li, M.H., Yan, W.C., Guo, X., Li, D.Z., Chen, Y.P., Ma, Y., Zhao, J.R., Li, Y.F., Zhang, J., and Chen, L.M., *Rev. Sci. Instrum.,* 2014, vol. 85, p. 113304. https://doi.org/10.1063/1.4901519
8. Ivanov, K., Uryupina, D.S., Volkov, R.V., Shkurinov, A.P., Ozheredov, I.A., Paskhalov, A.A., Eremin, N.V., and Savel'ev, A.B., *Nucl. Instrum. Methods. Phys. Res. A,* 2011, vol. 653, p. 58. https://doi.org/10.1016/j.nima.2011.01.160
9. Hollinger, R., Bargsten, C., Shlyaptsev, V.N., Kaymak, V., Pukhov, A., Capeluto, M.G., Wang, S., Rockwood, A., Wang, Y., Townsend, A., Prieto, A., Stockton, P., Curtis, A., and Rocca, J.J., *Optica,* 2017, vol. 4, p. 1344. https://doi.org/10.1364/optica.4.001344
10. Ivanov, K.A., Gozhev, D.A., Rodichkina, S.P., Makarov, S.V., Makarov, S.S., Dubatkov, M.A., Pikuz, S.A., Presnov, D.E., Paskhalov, A.A., Eremin, N.V., Brantov, A.V., Bychenkov, V.Y., Volkov, R.V., Timoshenko, V.Y., Kudryashov, S.I., and Savel'ev, A.B., *Appl. Phys.,* 2017, vol. 123, p. 252. https://doi.org/10.1007/s00340-017-6826-4

11. Wenz, J., Schleede, S., and Khrennikov, K., *Nat. Commun.,* 2015, vol. 6, p. 7568. https://doi.org/10.1038/ncomms8568
12. Hansheng Ye, YuqiuGu, Quanping Fan, Xiaohui Zhang, Shaoyi Wang, Fang Tan, Jie Zhang, Yue Yang, Yonghong Yan, Jiaxing Wen, Yuchi Wu, Wei Lu, Wenhui Huang, and Weimin Zhou, *AIP Adv.,* 2023, vol. 13, p. 035330. https://doi.org/10.1063/5.0130819
13. Balovnev, A.V., Grigor'eva, I.G., and Salakhutdinov, G.Kh., *Instrum. Exp. Tech.,* 2015, vol. 58, no. 2, pp. 252–257. https://doi.org/10.1134/S0020441215020049
14. Stafford, A., Safronova, A.S., and Faenov, A.Y., *Laser Part. Beams,* 2017, vol. 35, p. 92. https://doi.org/10.1017/S026303461600077X
15. Eftekhari-Zadeh, E., Blumcke, M.S., Samsonova, Z., Loetzsch, R., Uschmann, I., Zapf, M., Ronning, C., Rosmej, O.N., Kartashov, D., and Spielmann, C., *Phys. Plasmas,* 2022, vol. 29, p. 013301. https://doi.org/10.1063/5.0064364
16. Balovnev, A.V., Grigor'eva, I.G., and Salakhutdinov, G.Kh., *Instrum. Exp. Tech.,* 2015, vol. 58, no. 1, pp. 98–102. https://doi.org/10.1134/S002044121501025X
17. Efimov, N.E., Grigoryeva, I.G., Makarov, A.A., Krat, S.A., Prishvitsyn, A.S., Alieva, A.I., Savelov, A.S., Kirko, D.L., and Salakhutdinov, G.Kh., *Instrum. Exp. Tech.,* 2023, vol. 66, no. 2, p. 257–263.
18. Tilikin, I.N., Shelkovenko, T.A., Pikuz, S.A., Grigoryeva, I.G., Makarov, A.A., and Salakhutdinov, G.Kh., *Instrum. Exp. Tech.,* 2023, vol. 66, no. 4, pp. 600–604.
19. Balovnev, A.V., Grigoryeva, I.G., and Salakhutdinov, G.Kh., *Instrum. Exp. Tech.,* 2018, vol. 61, no. 1, pp. 91–94. https://doi.org/10.1134/S0020441218010128
20. Grigorieva, I.G., Makarov, A.A., Korf, A.N., and Salakhutdinov, G.Kh., *Instrum. Exp. Tech.,* 2022, vol. 65, no. 4, pp. 621–625. https://doi.org/10.1134/S002044122204011X
21. Malka, G. and Miquel, J., L, *Phys. Rev. Lett.,* 1996, vol. 77, p. 75. https://doi.org/10.1103/PhysRevLett.77.75
22. Beg, F.N., Bell, A.R., Dangor, A.E., Danson, C.N., Fews, A.P., Glinsky, M.E., Hammel, B.A., Lee, P., Norreys, P.A., and Tatarakis, M., *Phys. Plasmas,* 1997, vol. 4, p. 447. https://doi.org/10.1063/1.872103
23. Reich, Ch., Gibbon, P., Uschmann, I., and Föorster, E., *Phys. Rev. Lett.,* 2000, vol. 84, p. 4846. https://doi.org/10.1103/PhysRevLett.84.4846
24. Ivanov, K.A., Shulyapov, S.A., Turinge, A.A., Brantov, A.V., Uryupina, D.S., Volkov, R.V., Rusakov, A.V., Djilkibaev, R.M., Nedorezov, V.G., Bychenkov, V.Yu., and Savel'ev, A.B., *Contrib. Plasma Phys.,* 2013, vol. 53, p. 116. https://doi.org/10.1002/ctpp.201310023
25. Horst, F., Fehrenbacher, G., Radon, T., Kozlova, E., Rosmej, O., Czarnecki, D., Schrenk, O., Breckow, J., and Zink, K., *Nucl. Instrum. Methods. Phys. Res. A,* 2015, vol. 782, p. 69. https://doi.org/10.1016/j.nima.2015.02.010

Translated by N. Goryacheva